J1.3 Variability of Georgia and Florida air quality as a function of radar derived aerosol coverage and height.

Thomas Jones* and Sundar A. Christopher
Department of Atmospheric Science
The University of Alabama in Huntsville
Huntsville, AL

Abstract

Understanding the vertical distribution of aerosols is critical for air quality and other climate applications. Since current tools for obtaining this information have limited spatial and temporal coverage, we explore the use of radar data for obtaining injection heights of biomass burning aerosols produced from intense fires in southern Georgia during spring 2007. Using over 3 days of WSR-88 radar data from Jacksonville Florida between 23 – 27 May 2007, we quantify smoke injection heights using a modified severe storm algorithm products. Our analysis indicates that the maximum injection height is ~5 km for the strongest fire on 24 May, with an overall mean injection height > 3 km. Radar data are also capable of providing the diurnal variation of aerosol heights, which is shown to be related to variations in downstream air quality. This research represents the initial step in a much longer term effort aimed at improving future air quality forecasting applications through statistical and numerical modeling.

1. Introduction

One of the major outstanding issues in air quality monitoring and forecasting is the lack of accurate measurements of the vertical distribution of aerosols, which is vital to local and downstream air quality conditions (e.g. Engel-Cox et al. 2006; Wang et al. 2006). What data are available generally originate from case study experiments or localized lidar locations. Recently, Kahn et al. (2007) has

 * Corresponding author address: Thomas A. Jones University of Alabama in Huntsville, 320 Sparkman Dr. Huntsville, AL 35805. *email: tjones@nsstc.uah.edu*

proposed the use of the Multiangle Imaging Spectroradiometer (MISR) instrument currently aboard the Terra EOS polar orbiting satellite to determine injection height that could be useful for numerical modeling simulations (Wang et al., 2006). MISR has a narrow swath width limiting global measurements to once every 9 days. In additional to total column aerosol optical thickness (AOT), the MISR level 2 stereo height product can resolve the vertical distribution of aerosols (Moroney et al. 2002). The launch of the Cloud-Aerosol Lidar and Infrared Pathfinder Satellite Observation (CALIPSO) satellite and its accompanying downward pointing lidar, which is sensitive to both aerosol and cloud layers, provides another source of data for aerosol profiles (Vaughan et al. 2004). However, its small swath width (~50 km) limits coverage of any one location to once every 16 days. Since the overall temporal and spatial coverage of these data are limited, analysis of short-term trends in the vertical distributions of aerosols and their affects on downstream air quality has proven problematic.

On a regional scale, changes in air quality are both a function of local aerosol sources and aerosols transported from great distances from the original source. One example is aerosols from biomass burning fires that can loft large amounts of particulate matter several kilometers into the atmosphere as a result of localized instability and increased buoyancy produced by the intense heat of the fire (Banta et al. 1992). These aerosols can also be lifted above the boundary layer, where they can be transported hundreds of kilometers downstream before descending

1

and lowering surface air quality. The maximum height to which substantial aerosols are lifted at the source is known as the injection height (e.g. Penner et al. 1994). If this parameter is known, then the probability of skillful air quality forecasts downstream of a fire event are significantly increased (e.g. Colarco et al. 2004; Wang et al. 2006). However, there remain few objective, near real-time observations of injection height, requiring greater creativity in the use of currently available observation tools.

One currently under-utilized tool for sampling injection height is radar. For intense biomass burning, concentrations and sizes of particulate matter lofted into the atmosphere are large enough to be detected by precipitation radars such as the Weather Surveillance Radar-1988 Doppler (WSR-88D) network in the United States. We analyze data between 23 – 27 May 2007 in southern Georgia to access the ability of WSR-88D radars at sampling and quantifying injection height (Hufford et al. 1998). This time period represents a subset of a two month long fire event occurring in the southeastern United States between mid-April and mid-June 2007. We first combine radar data with aerosol observations from the Moderate Resolution Imaging Spectroradiometer (MODIS) and CALIPSO instruments to first define the injection height of a smoke plume. When then use the time-series of radar derived injection heights to access the importance of height and time information of smoke plume characteristics to downstream surface air quality ($PM_{2.5}$) measurements.

2. Data & Methodology

The WSR-88D network consists of approximately 140 operational radars spread out throughout the United States operated by the NOAA National Weather Service. The WSR-88D is an active S-Band (10 cm) precipitation radar, with a radial resolution of 1° and a range bin of 1 km providing a 3-D

data volume every 5 to 6 minutes (Crum and Alberty 1993). A WSR-88D may be operated in one of several Volume Coverage Patterns (VCPs) that define the number and height of each scan elevation encompassing a single volume of data (Crum and Alberty 1993; Brown et al. 2000a). The WSR-88D was designed to detect precipitation sized hydrometeors (D > 100 μm) out to a range of 230 km from backscattered electromagnetic energy in the microwave spectrum. Returned energy is converted into water equivalent reflectivity (dBz), which is proportional to the sixth power of an object's diameter. As a result, small concentrations of large objects will result in higher reflectivity values compared to large concentrations of small objects. Velocity relative to the radar (radial velocity, ms^{-1}) is retrieved by sampling the Doppler shift of the returned radar pulse (Doviak and Zrnic 1993). Precipitation radars are generally not sensitive to the smoke aerosols themselves, which generally have diameters less than 1 μm. However, intense fires also loft large amounts of ash and partially carbonized debris into the atmosphere, that *are* detectable by a precipitation radar (Banta et al. 1992). We use radar reflectivity and velocity characteristics of the observed ash and large particulate matter to estimate the spatial and vertical distributions of smoke aerosols.

We obtained over 3 days (22 UTC 23 May to 00 UTC 27 May) of level-2 WSR-88D radar data from the Jacksonville, FL radar (KJAX) to sample smoke plumes produced by the fires in GA. Fire locations were obtained from the geostationary Wildfire Automated Biomass Burning Algorithm (WFABBA) product from GOES-12 (Prins et al. 1994). The major fires are located approximately 80-100 km west-northwest of the radar location. During this period, the radar was operated primarily in two precipitation modes: VCP-12; prior to 9 UTC 24 May; and VCP-21 thereafter. Figure 1 shows the height above

mean sea level of the beam centerline for all elevations of VCP-12 (a) and VCP-21 (b). Recall that the fires are located between 80 and 100 km from the radar at this time, which means that smoke and ash must exceed at least ~1.5 km in height to be detectible by the lowest elevation scan (0.5º) plotted in Figure 1.

To objectively determine injection height from WSR-88D data, we use a modified version of the Storm Cell Identification and Tracking (SCIT) algorithm, which was designed to detect and report spatial and temporal characteristics of individual storm cells (Johnson et al. 1998). Fortunately, intense smoke plumes often exhibit similar characteristics to those observed in supercell thunderstorms, just on a smaller and less intense scale. To detect smoke plumes, we modified SCIT to detect "storms" using reflectivity thresholds as low as 10 dBz compared to the 30 dBz value used operationally. This increases the algorithm's sensitivity to the weaker reflectivity returns associated with smoke plumes.

During this period, no significant precipitation features were present after 22 UTC 23 May near the location of the fires based on subjective analysis of the radar and other meteorological data available. To ensure that the detections produced by SCIT are indeed from smoke plumes, we compared their location with GOES-fire pixels using a 15 km, ±30 minute search radius, similar in concept to the "SCIT-filter" (Jones et al. 2004). In addition, SCIT detections with a maximum reflectivity > 45 dBz were removed and reflectivity exceeding this value is very likely to be a result of precipitation. We make use of the "storm-top" parameter from the SCIT algorithm, which reports the highest level (in km) for which 10-dBz or greater reflectivity values were observed corresponding to an overall storm detection. Unless otherwise noted, all height levels reported here have been converted to height above mean sea level (ASL) for consistency across all sensors.

There exists significant uncertainty in the SCIT derived "storm-top" heights and their relationship to aerosol injection height. The first is solely a function of radar geometry. As the radar pulse travels outward from a radar, its height above the ground also increases as observed in Figure 1. Under normal atmospheric conditions, radar beam bending can be approximated by Equation 1, where Z is the height of the beam at a certain range from the radar (R), r_e' is 4/3 earth's radius, θ is the elevation angle in degrees, and Z_o is the height of the radar above sea level (Rinehart 2004).

$$Z = \sqrt{R^2 + r_e'^2 + 2Rr_e' \sin(\theta)} - r_e' + Z_o \qquad (1)$$

At a range of 100 km, few observations of phenomena are possible below 2 km under normal atmospheric conditions. However, both VCPs are able to detect phenomena exceeding 10 km in height at this range. Uncertainty in reported height values is a result of how they are calculated. Maximum storm height is defined as the height of the beam centerline for which the highest reflectivity was observed at the range of the detection. At 100 km range, the uncertainty in storm top estimate (for targets < 10 km in height) has been estimated to be approximately ±1 km (Howard et al. 1997; Brown et al., 2000b). During the nighttime, when the boundary layer is lower and fires are generally less intense, this radar will have difficulty observing smoke plume characteristics at ranges of 100 km or more.

We also must emphasize that we are not sampling smoke aerosols directly, but the larger biomass matter produced by the fire and lofted into the atmosphere by the fire (Banta et al., 1992). Some of this burnt biomass may have diameters up to 1 cm, accounting for much of the observed reflectivity. However, the lifetime of such large biomass matter in

3
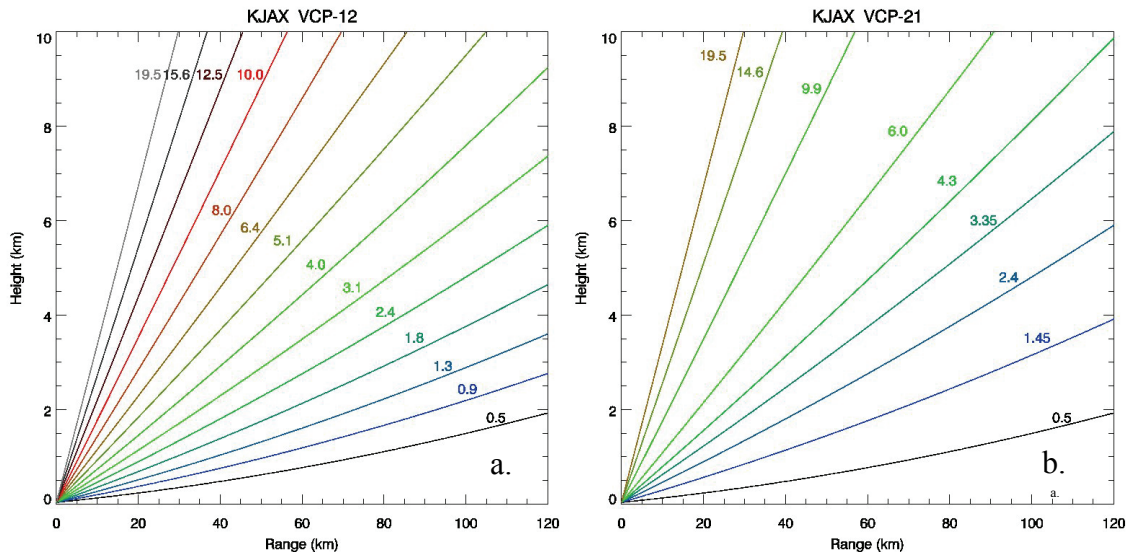
Figure 1. Centerline heights (above sea level) for all elevation scans used by VCP-12 (a) and VCP-21 (b) as a function of range from the KJAX radar using Equation 1.

the atmosphere is generally on the order of minutes before falling back to the ground (Hufford et al. 1998). Conversely, aerosols remain in the atmosphere for much longer periods of time. Thus, radar derived injection height estimates are likely underestimates of the true height to which some aerosols reach. Smoke aerosols are much smaller and lighter than the particles associated with the radar reflectivity returns (e.g. Hufford et al. 1998). As a result, smoke aerosols are likely being transported higher into the atmosphere than indicated by the SCIT derived heights or the radar cross section presented below. Just how much we are underestimating *aerosol* injection height will require further research.

MODIS level 1B reflectance and level 2 aerosol data (Levy et al. 2007) from the Terra and Aqua satellites are qualitatively compared with the radar data, to determine the implications of large amounts of smoke aerosols being injected into the atmosphere on downstream aerosol and air quality conditions. The HYbrid Single-Particle Lagrangian Integrated Trajectory (HYSPLIT) model is used to model the trajectory of parcels at multiple levels from one location backwards or forwards in time (Draxler 2003). Finally,

we compare the radar results with a single CALIPSO lidar overpass at 1914 UTC on 24 May 2007. CALIPSO does not overpass the fire affected region at ideal times for quantitative comparison of aerosol vertical profiles, but is close enough to at least provide insight as to where the aerosols being injected into the atmosphere. The primary source for surface air quality data will be $PM_{2.5}$ measurements from the EPA Aerometric Information Retrieval System (Watson et al. 1998). Most sites make use of Tapered-Element Oscillating Microbalance (TEOM) instruments which report $PM_{2.5}$ concentrations on an hourly averaged basis with an overall accuracy of ±1.5 μg m^{-3}. Hourly data are acquired and quality controlled using the AirNow air quality database.

3. Results
a. Overview

Regional aerosol and cloud characteristics at 1640 and 1815 UTC on 25 May derived from Terra and Aqua MODIS level 1B and level 2 aerosol data are given in Figure 2. No aerosol retrievals could be made near the fire locations, (denoted as red 'X's), due to the presence of a large low-level
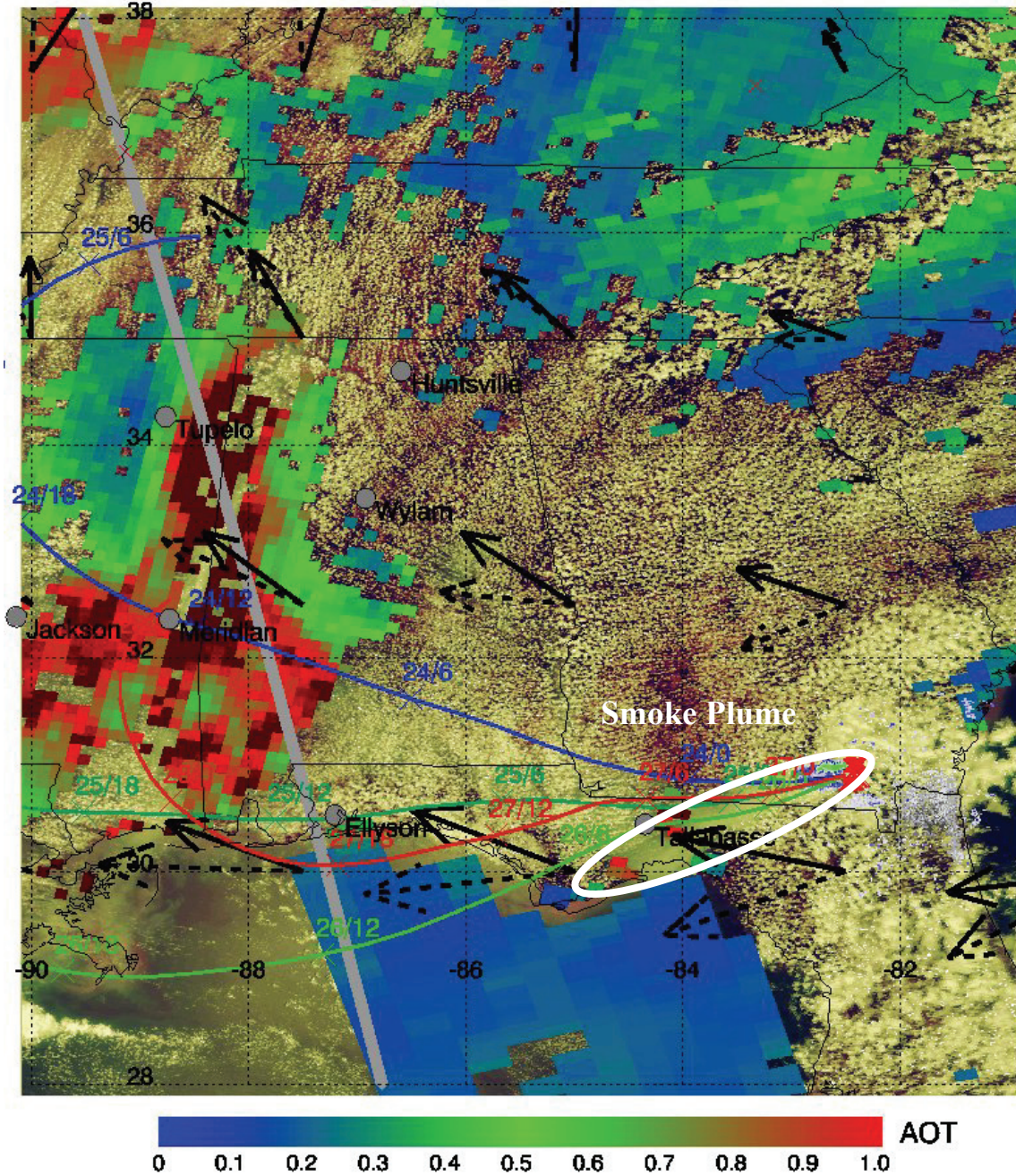
Figure 2. MODIS false color image with MODIS level 2 AOT overlaid where valid retrievals occur. Note that clouds prevent aerosol retrievals near where the fires are located. Wind vectors at 850 hPa (dashed) and 700 hPa (solid) levels at 00 UTC 25 May are shown and indicate a general east to west flow. GOES fire pixels for 24 May 2007 are plotted as red 'X's. The grey line represents the CAPLISO overpass from 1914 UTC on 24 May. Foward-trajectory analysis from HYSPLIT initialized at 21 UTC for 23 – 26 May originating at the location of the fires are also plotted and labeled at 6 hour intervals. Note that parcels generally travel in an east to west direction for during all four days.

cumulus cloud field. However, substantial aerosol concentrations (AOT > 1.0) were retrieved in western AL and eastern MS, downstream of the fire as evident by the 850 and 700 hPa level wind vectors. Also shown are the GOES fire pixels from 24 May and WSR-88D reflectivity at 1812 UTC 24 May. Note the small spatial coverage of the fires and radar observable plume compared to the much larger downwind coverage of high AOT. The smoke plume itself is visible using the MODIS L1B data, extending from the fire locations downwind to the west-southwest into FL.

Reflectivity from the KJAX WSR-88D radar at 1812 UTC (approximately 1:18 p.m. local time) at 1.5 km in altitude is shown in Figure 3a. The radar data in this plot was placed on Cartesian grid at a horizontal resolution of 1 km and a vertical resolution of 500 m. Two distinct fire plumes are evident 80-100 km west-northwest of the radar, which are labeled F1 and F2. A third, much weaker fire is present ~50 km northwest of the radar (F3). The locations of these fire plumes correspond well with the GOES fire pixels at this time, though the radar-derived plumes are somewhat downwind of the fire pixels, as expected. The northernmost fire (F1) appears to be the strongest, with higher reflectivity values corresponding to a larger coverage of detectable burnt biomass. All smoke plumes are oriented in an east to west direction corresponding with the east to west wind flow present at this time in the vicinity of the radar (Fig. 2). Analysis of the velocity characteristics of the plumes indicate that they were traveling away from the radar between 5 and 10 ms^{-1} with wind speed increasing as a function of height.

F1 is visible at the 2.4º elevation scan for a period of several hours, which corresponds to a height > 4 km at ranges > 80 km (Fig. 1). F2 generally exhibits weaker and lower reflectivity values. This can be visualized by examining a vertical cross section of radar data through the smoke plume of both fires at this time (Fig. 3b). F1 is associated with greater reflectivity values at all levels and indicates > 5 dBz returns to almost 6 km in altitude, well above the boundary layer height at this time. The large reflectivity values associated with the northern fire (> 30-dBz) indicate that very large concentrations of burnt bio-matter and their associated aerosols are being lofted high into the atmosphere, in response to localized instability produced by the heat of the fires.

b. Injection Height Analysis

We objectively quantify injection height between 22 UTC 23 May and 00 UTC 27 May using SCIT output from every volume scan, filtered to remove precipitation and other non-smoke related detections. Several interesting trends are apparent in the time series of injection height (Fig. 3c). First is that the detections are split up into four separate temporal groupings, the first between 22 UTC 23 May and 4 UTC 24 May, the second between 15 UTC 24 May and 1 UTC 25 May, the third between 18 UTC 25 May and 4 UTC 26 May, and the last after 18 UTC 26 May (Fig. 3c). These groups correspond to the late afternoon and early evening time period locally, when convective turbulence and boundary layer height are maximized. During the first period, detected injection heights are clustered around 2.5 to 3 km, with few significant differences (> 1 km) in injection height between the two larger fires observed. Small differences are primarily a function of range from the radar. If lofted bio-matter is detected at the 1.45º elevation at 80 and 100 km, the latter will have a higher smoke cell height, assuming no reflectivity returns at higher elevation scans. This does increase uncertainty associated with this technique, especially when only data from a single radar are used.

During the nighttime hours, the intensity of the fires decreases, and the lower

6
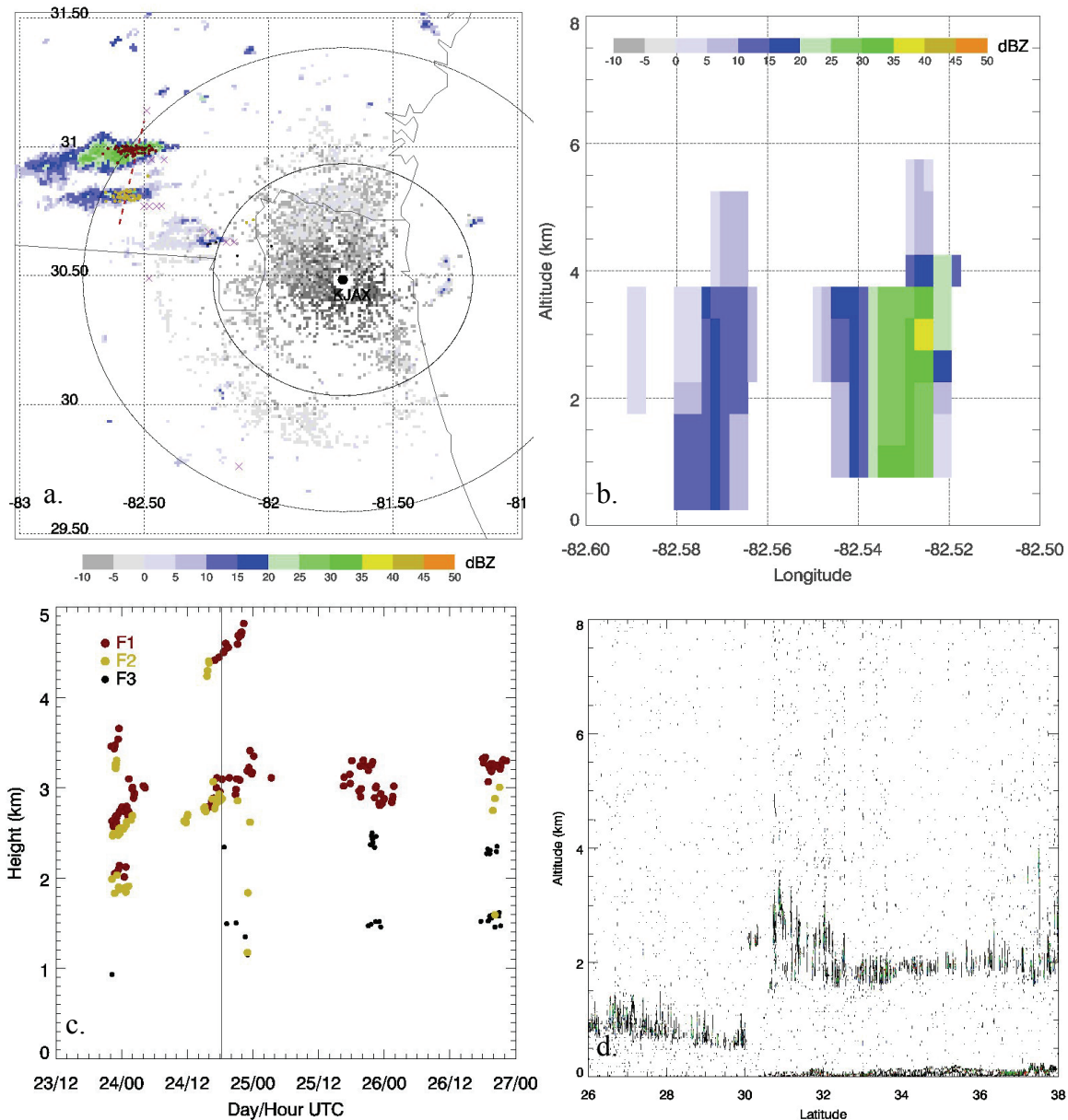
Figure 3. KJAX Reflectivity at 1.5 km at 1812 UTC 24 May showing two distinct smoke plumes in southern GA, northwest of the radar (a). Circles indicate 50 and 100 km range rings centered around the radar location. SCIT smoke detections are overlaid. Vertical cross section of reflectivity (b), corresponding to the dashed line in (a). Note the northern fire has substantially greater reflectivity at all levels with 10 dBz returns extending to 5 km in altitude. Time series vs. height of SCIT smoke-cell detections between 22 UTC 23 May and 00 UTC 27 May (c). Injection heights for northern fire (F1) are plotted in dark red, while those from the southern fire (F2) are plotted in yellow. CALIPSO 532 nm backscatter reflectance as a function of latitude for 1914 UTC on 24 May 2007 (d). Aerosol layer is readily apparent around 2 km ASL from near the Gulf Coast (31ºN) to Northern MS (36ºN).

atmosphere becomes increasingly stable due to cooling surface temperatures. As a result, SCIT no longer detects smoke plumes during this period. Subjective analysis of the radar data during this time also shows very little evidence for the fires, indicating that the amount of aerosols being lofted into the atmosphere is much less than during the daytime hours. After 15 UTC on 24 May, the intensity of the fires begins to increase again. Initial injection height detections are approximately 3 km ASL, similar to the previous time period. However, detections reaching up to 4.5 km are soon evident, placing the biomass and aerosols well above the ambient boundary layer height. Initially, these are from the southern fire (yellow), but soon after detections at this altitude result solely from the northern fire (dark red). Note that injection heights at both ~3 km and 4.5 km levels were recorded with F1. This difference is a function of the SCIT algorithm finding 10 dBz reflectivity associated with a smoke plume from either the 1.45º or 2.4º elevation data. At the time of the radar cross section (1812 UTC), the injection height for F1 was 4.5 km, which is consistent with Figure 3b. The variability in injection height for a single plume is not unexpected and reflects the extreme temporal variability of aerosol concentrations near the fire source. Maximum injection height for F1 remains ~4.5 km until approximately 00 UTC 25 May. Both fires decrease in intensity rapidly thereafter, with only a single detection after 1 UTC. A few smoke plume detections were obtained from F3 closer to the radar, with heights only reaching ~1 km. Both radar data and GOES fire data indicates that this fire is much weaker; thus, is less likely to transport significant aerosol concentrations into the free atmosphere (i.e. above the boundary layer).

These patterns are repeated for the afternoons of 25 and 26 May, with radar derived injection heights near 3 km observed both days. However, both radar and GOES

data indicate that F2 becomes less intense following 25 May, while the relatively small and weak F3 becomes somewhat more intense. No smoke plume detections were made on F2 between 18 UTC 25 May and 4 UTC 26 May, which only three detections occurring the next afternoon (Fig. 3c). Conversely, the number of injection height detections for F3 in excess of 2 km increases from one prior to 25 May to ~10 for both the afternoons of 25 and 26 May. The largest fire, F1, remains strong throughout this period, with many smoke plume detections in excess of 3 km associated with it at all times.

c. Comparison with CALIPSO

Unfortunately, no CALIPSO overpass occurred directly over the fire locations to allow a full quantitative assessment of radar-derived injection heights. However, an overpass did occur in western AL at 1914 UTC on 24 May, showing a substantial aerosol layer near 2 km ASL, corresponding to the boundary layer height at this time (Fig. 3d). To determine the source of these aerosols, the HYSPLIT model along with meteorological data archives from the Air Resources Laboratory were used to calculate the trajectory of an atmospheric parcel from a point in western AL (32.5ºN, -88.0ºW) at 1900 UTC 24 May at 2 km in altitude backwards in time 24 hours. The modeled trajectory traces back to a point near the GA fires at approximately 03 UTC 24 May. Parcel height increases as one travels from the initialization location to regions nearer the fires indicating that lower-level air quality is being impacted by aerosols originating from a higher level. Recall that the radar derived injection height prior to 03 UTC 24 May was around ~3 km. This agrees well with the HYSPLIT analysis that shows a parcel being injected near 3 km in height at 03 UTC 24 May near the fire descends to ~2 km where CALIPSO observes the aerosol layer in western AL at 19 UTC.

d. Relationship to air quality

To compare downstream air quality with radar derived injection height, we selected 7 air quality measurement stations including Tallahassee, FL; Ellyson, FL; Wylam, AL; Huntsville, AL; Meridian, MS; Tupelo, MS, and Jackson, MS (Fig. 4). HYSPLIT trajectory analysis was initiated at 21 UTC on 23 – 26 May at 2 km in altitude and run for 36 hours. The trajectories for all four days clearly indicate a westward transport of aerosols from southern GA, into far western FL, and far southern AL (Fig. 2). Trajectories turn northward in southern MS in response to high pressure system centered in the upper Midwest. These trajectories correspond well with the MODIS AOT values for 25 May, which are maximized in eastern MS.

To determine the relationship between radar derived injection heights and surface air quality, we compile a time series of hourly $PM_{2.5}$ data for the seven selected sites, which are plotted in Figure 4 along with radar derived injection heights between 22 UTC 23 May and 00 UTC 27 May. Recall that a strong diurnal cycle is apparent in injection height with values between $2 – 3$ km observed during the later afternoon and early evening hours each day, with values near 5 km observed on 24 May (Fig. 3c). Air quality at Tallahassee, FL shows a similar diurnal cycle, with $PM_{2.5}$ maximized during the same time period as maximum injection heights were also recorded (Fig. 2). Air quality at this site lowest (highest $PM_{2.5}$) on 25 May, which is due to strong substance present along the parcel trajectory. Substantial temporal variability was also observed in $PM_{2.5}$, which is a direct response to a similar variability in the characteristics of the fires themselves. Since this site is in the direct path of the smoke plume with a transport time of less than 6 hours required to affect air quality, the strong correlation between the radar derived smoke data and $PM_{2.5}$ was expected. Air quality nearer the fire will often be lower than that recorded much further away. Given the time necessary to transport smoke from the fire to an air quality measurement site, a temporal lag should exist between radar derived smoke properties and $PM_{2.5}$.

Further downstream, the effect of smoke on air quality becomes more complex. In Ellyson, which is located in the far western Panhandle of FL, $PM_{2.5}$ modest peaks of ~40 $\mu g \ m^{-3}$ were observed compared to a background value of ~15 $\mu g \ m^{-3}$ around 12 UTC for both 24 and 25 May. These peaks occur roughly twelve hours after the previous peak fire activity, which agrees well with the parcel transport speed indicated by HYSPLIT, especially on 25 May. After this peak, little change in $PM_{2.5}$ concentrations was observed, with HYSPLIT and MODIS AOT data indicating that most of the smoke is transported further south into the Gulf of Mexico before curving back north into MS. Also, Ellyson is very near the Gulf Coast, where localized sea-breezes may cleanse the atmosphere, which may partially explain the lower $PM_{2.5}$ values observed here compared to locations further downstream in MS.

At Tupelo, which is located in northeastern MS, two peaks in $PM_{2.5}$ are present. One occurs between $12 – 18$ UTC 24 May and the second higher peak occurring between 18 UTC 25 May and 06 UTC 26 May (Fig. 4). The first occurs approximately $12 – 18$ hours after the radar derived fire detections late on 23 May, which is consistent with the trajectory analysis. The latter period appears to be a result of aerosol convergence as from those produced during 24 and 25 May, since trajectories for these days remain well south of Tupelo. These peaks occur over a longer time period and are "smoother" than observed at Tallahassee as a result of mixing and overall broadening of the smoke plume. Interestingly, $PM_{2.5}$ trends at Meridian and Jackson are much less apparent. Further examination of the atmospheric conditions for these areas will be required to determine the cause. Relatively
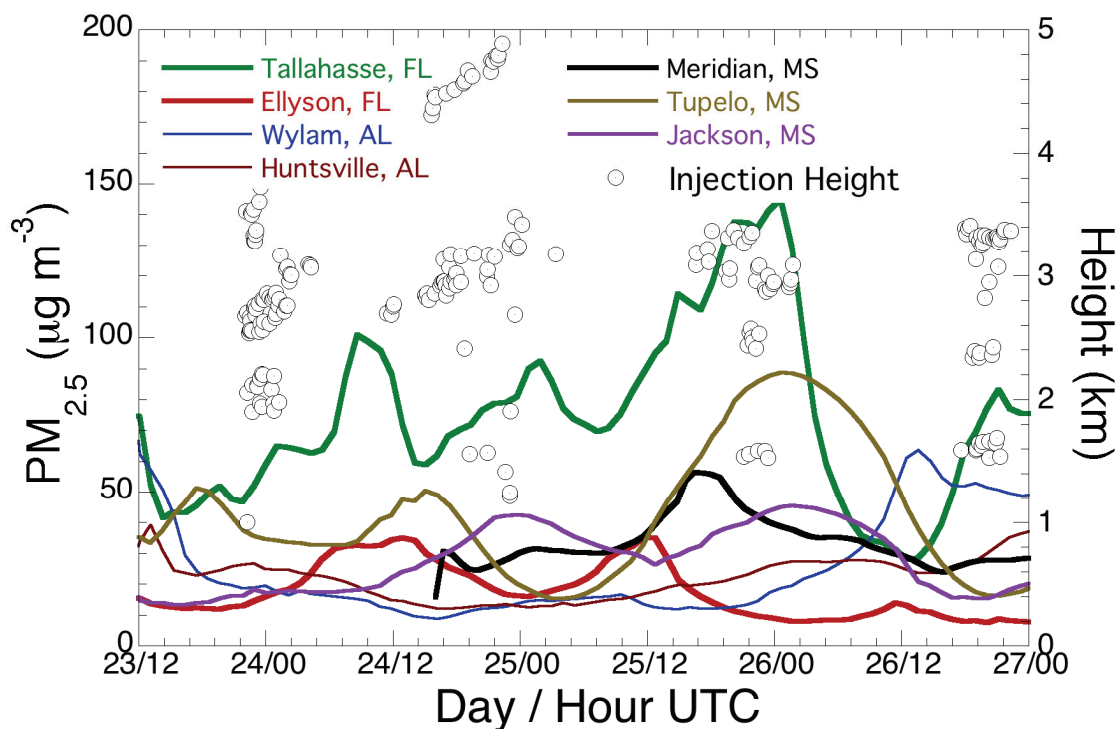
Figure 4. Time series from 12 UTC 23 May to 00 UTC 27 May of hourly PM$_{2.5}$ (µg m^{-3}) for Tallahassee, FL; Wylam, AL; Huntsville, AL; Meridian, MS; Tupelo, MS, and Jackson, MS. Also plotted are radar derived injected height values from the KJAX radar for the same period.

low PM$_{2.5}$ values were recorded at stations in AL, which is expected as both trajectory and aerosol data indicate that smoke is being transported far to the south of these sites. Finally, there are also examples where wind and stability conditions are such that smoke aerosols may be pooled and concentrated over a small area quite far downstream. We will analyze where this phenomena is related to the smoke plume itself, or is primarily a function of the prevailing wind conditions in future research.

While the relationship between the diurnal variation in injection height and downstream changes in air quality is clearly evident, it remains difficult to precisely quantify injection vs. air quality at a specific time (Fig. 4). The radar data does confirm that aerosols are being injected into the free atmosphere in large quantities during the late afternoon hours. Satellite AOT and surface PM$_{2.5}$ data also indicate that these aerosols are

being transported long distances downstream; however, it is difficult to quantify the precise relationship between injection height at a certain time and downstream air-quality at another time. To accomplish this, the injection height – air quality relationship will have to be analyzed as a function of many meteorological conditions along the path from the fire source to the air quality measurement site, which will be a priority for future research.

4. Conclusions

Using WSR-88D radar data, we show that it is possible to estimate the injection height of bio-matter into the atmosphere from intense biomass burning, which is in turn useful in studies of particulate matter air quality and numerical modeling simulations that require such information (Wang et al. 2006). A modified version of the SCIT algorithm was able to objectively calculate 10 dBz injection heights for several fires in

southern GA between 23 – 27 May. The intensity of the fires showed a strong diurnal variability with the strongest reflectivity observed during the late afternoon and evening hours. SCIT derived bio-matter injection heights ranged between 3 and 5 km above sea level for the two most significant fires. The strongest (northern) fire generated measurable reflectivity above 5 km for a several hour period between 17 UTC 24 May and 00 UTC 25 May. Analysis of MODIS aerosol optical thickness indicates that the smoke from these fires was transported into western AL and Eastern MS between 12 UTC 24 May and 12 UTC 25 May. According to HYSPLIT modeled parcel trajectories, at least a portion of the aerosol layer observed by CALIPSO originates from the fire region located more than 500 km away ~18 hours previously, from a height at ~3 km. This is in excellent agreement with the SCIT derived plume heights reported at this time. The relationship between the diurnal variation of injection height and air quality is substantial for sites near and downstream of the fires. For sites not in the direct path of the smoke plume, very little variability in air quality was observed.

Several sources of uncertainty remain before radars can be used to determine aerosol injection height with a high degree of certainty. The foremost limitation is a result of radar beam bending as a function of range. As range increases, the uncertainty in height measurements also increases, while the sensitivity to low-level phenomena decreases. Future research will utilize data from multiple radars to at least partially overcome this problem and to also retrieve the 3-D wind field associated with each smoke plume. The question also remains as to whether or not the 10-dBz threshold is a good indicator of injection height. Currently, combined aerosol profile, S-Band radar reflectivity datasets do not exist to quantitatively make this comparison, but time will eventually provide the necessary data. Overall, this research provides a framework for the use of widely available radar date, as an independent source, to estimate the height smoke aerosols are being injected into the atmosphere from biomass burning and comparing height information to downstream air quality.

Acknowledgements

References

Banta, R. M., L. D. Olivier, E. T. Holloway, R. A. Kropfli, B. W. Bartram, R. E. Cupp, and M. J. Post, (1992), Smoke-column observations from two forest fires using Doppler lidar and Doppler radar. *J. Appl. Meteor.*, 31, 1328-1349.

Brown, R. A., V. T. Wood, and D. Sirmans, (2000), Improved WSR-88D scanning strategies for convective storms, (2000), *Wea. and Forecasting*, 15, 208-220.

Brown, R. A., J. M. Janish, and V. T. Wood (2000b), Impact of WSR-88D scanning strategies on severe storm algorithms. *Wea. and Forecasting*, 15, 90-102.

Colarco, P. R., M. R. Schoeberl, B. G. Doddridge, L. T. Marufu, O. Torres, and E. J. Welton (2004), Transport of smoke from Canadian forest fires to the surface near Washington, D.C.: Injection height, entrainment, and optical properties, *J.*

Geophys. Res., 109, D06203, doi:10.1029/2003JD004248.

Crum, T. D., and R. L. Alberty (1993), The WSR-88D and the WSR-88D Operational Support Facility. *Bull. Amer. Meteor. Soc.*, 74, 1669-1687.

Doviak, R.J., and D. S. Zrnic (1993), Doppler radar and weather observations: Second edition.
Academic Press, San Diego CA, 562 pp.

Draxler, R. R. (2003), Evaluation of an ensemble dispersion calculation. *J. Appl. Meteor.*, 42, 308-317.

Engel-Cox J. A., Hoff, R. M., Rogers, R., Dimmick, F., Rush, A. C., Szykman, J. J., Al-Saadi, J., Chu, D. A., Zell, E. R., 2006. Integrating lidar and satellite optical depth with ambient monitoring for 3-dimensional particulate characterization. *Atmospheric Environment*, 40, 40, 8056-806.

Howard, K. W., J. J. Gourley, and R. A. Maddox, (1997), Uncertainties in WSR-88D measurements and their impacts on monitoring life cycles. *Wea. and Forecasting*, 12, 166-174.

Hufford, G. L., H. L. Kelley, W. Sparkman, and R. K. Moore (1998), Use of real-time multi-satellite and radar data to support forest fire management., *Wea. and Forecasting*, 13, 592-605.

Kahn, R. A., W. H. Li, C. Moroney, D. J. Diner, J. V. Martonchik, and E. Fishbein (2007), Aerosol source plume physical characteristics from space-based multiangle imaging. *J. Geophys. Res.*, 112, D05S17, doi:10.1029/2006JD007647.

Johnson, J. T., P. L. MacKeen, A. Witt, D. Mitchell, G. J. Stumpf., M. D. Eilts, and K. W.

Thomas, (1998), The Storm Cell Identification and Tracking algorithm: An enhanced WSR-88D algorithm, *Wea. and Forecasting*, 13, 263-276.

Jones, T. A., K.M. McGrath, and J.T. Snow, (2004), Association Between NSSL Mesocyclone Detection Algorithm detected vortices and tornadoes. *Wea. and Forecasting*. 19, 872-890.

Kahn, R. A., W. H. Li, C. Moroney, D. J. Diner, J. V. Martonchik, and E. Fishbein (2007), Aerosol source plume physical characteristics from space-based multiangle imaging. *J. Geophys. Res.,* 112, D05S17, doi:10.1029/2006JD007647.

Levy, R. C., L. A. Remer, S. Mattoo, E. F. Vermote, Y. J. Kaufman, (2007), Second-generation operational algorithm (2007a), Retrieval of aerosol properties over land from inversion of Moderate Resolution Imaging Spectroradiometer spectral reflectance *J. Geophys. Res.*,112, D13211,10.1029/2006JD007811.

Moroney, C., R. Davies, and J. P. Miller (2002), MISR stereoscopic image matchers: Techniques and results, *IEEE Trans. Geosci. Remote Sens.,* 40, 1547-1559.

Penner, J. E., R. J. Charlson, J. M. Hales, N. S. Laulainen, R. Liefer, T. Novakov, J. Ogren, L. F. Radke, S. E. Schwartz, and L. Travis (1994), Quantifying and minimizing uncertainty in climate forcing by anthropogenic aerosols, *Bull. Amer. Meteorol. Soc.*, 75, 375-400.

Prins, E.M. and W.P. Menzel, 1994: Trends in South American biomass burning detected with the GOES visible infrared spin scan radiometer atmospheric sounder from 1983 to 1991. *Jour. Geo. Res.*, **99**, 16,719-16735.

Rinehart, R. E. (2004), Radar for Meteorologists: Fourth Edition. Rinehart Publishing, Columbia, MO, 482 pp.

Vaughan, M., S. Young, D. Winker, K. Powell, A. Omar, Z. Liu, Y. Hu, and C. Hosteler, (2004), Fully automated analysis of space-based lidar data: an overview of CALIPSO retrieval algorithms and data products. *SPIE*, 5575, 16-30.

Wang, J., S. A. Christopher, U. S. Nair, J. S. Reid, E. M. Prins, J. Szykman, and J. L. Hand (2006), Mesoscale modeling of Central American smoke transport to the United States: 1. "Top-down" assessment of emission strength and diurnal variation impacts, *J. Geophys. Res.*, 111, D05S17, doi:10.1029/2005JD006416.

Watson, J.G., E. M. Fujita, J. C. Chow, B. Zielinska, L. W. Richards, W. Neff, and D. Dietrich (1998), Northern Front Range Air Quality Study Final Report, prepared for Colorado State University. *Cooperative Institute for the Research in the Atmosphere*, by Desert Research Institute, Reno, NV.